Volume 1 | Number 1 | Jan 2013 | Pages 1–100

Journal of
Materials Chemistry A

Materials for energy and sustainability
www.rsc.org/materialsA

Li⁺

ROYAL SOCIETY
OF CHEMISTRY

ROYAL SOCIETY
OF CHEMISTRY

www.rsc.org/materialsA

Liquid-Crystalline Ionic Liquids Modified Conductive Polymers as Transparent Electrode for Indium-Free Polymer Solar Cells

Shuqin Xiao[a], Lie Chen[a,b], Licheng Tan[a,b], Yiwang Chen[a,b]

[a]College of Chemistry/Institute of Polymers, Nanchang University, 999 Xuefu Avenue, Nanchang 330031, China

[b]Jiangxi Provincial Key Laboratory of New Energy Chemistry, Nanchang University, 999 Xuefu Avenue, Nanchang 330031, China

Corresponding author. Tel.: +86 791 83968703; fax: +86 791 83969561. E-mail: ywchen@ncu.edu.cn (Y.W. Chen)

Abstract

Ordered microstructure and high conductivity of poly(3,4-ethylenedioxythiophene): poly-(styrene sulfonate) (PEDOT:PSS, commercial product PH1000) films for transparent anode were obtained by liquid-crystalline ionic liquids modification. By spin-coating 1-hexadecyl-3-methylimidazolium hexafluorophosphate ([C$_{16}$MIm]PF$_6$) or 1-hexadecyl-3-methylimidazolium tetrafluoroborate ([C$_{16}$MIm]BF$_4$) on the PH1000 film, half of the insulating PSS on top surface of the PH1000 could be successfully removed and the PEDOT formed ordered and continuous molecular packing. The conductivity of the PH1000 dramatically increased from 0.4 S cm^{-1} to 1457.7 S cm^{-1} for PH1000/[C$_{16}$MIm]PF$_6$ and 1243.8 S cm^{-1} for PH1000/[C$_{16}$MIm]BF$_4$. At the same time, spontaneous orientation of the liquid-crystalline ionic liquids with liquid-crystallinity further promoted the ordered packing arrangement of both PH1000 and active layer. The power conversion efficiency based on PH1000/[C$_{16}$MIm]PF$_6$ and PH1000/[C$_{16}$MIm]BF$_4$ as anode is comparable to that obtained from the device with indium tin oxide (ITO) anode. In addition, liquid-crystalline ionic liquids modification is also good for the energy alignment, facilitating charge injection and transport, without any extra hole transport layer. Furthermore, these novel liquid-crystalline ionic liquids modification PH1000 anodes have potential applications in the fabrication of ITO-free large-area flexible printed polymer solar

cells.

1. Introduction

Polymer solar cells (PSCs) known as one of printed electronics, have received much attention in recent years, due to its advantages of light weight, mechanical flexibility, portability, potential for low-cost production of electronic devices fabricated by a continuous solution-based roll-to-roll process.[1,2] Up to now, the power conversion efficiency (PCE) of PSCs single cells is over 10%.[3,4] Currently, fabricating the high-performance devices mostly depend on indium tin oxide (ITO) as transparent electrodes. However, ITO has intrinsic problems such as high mechanical brittleness, scarce indium on earth, poor adhesion to organic and polymeric materials and inferior physical properties for high temperature treatment and so on.[5] Therefore, to meet the requirement of the roll-to-roll technique and commercialized production, there is a strong demand for new transparent conductivity materials to replace traditional ITO.

Many conductivity materials have been applied as transparent electrode in recent years, including conducting polymers,[6,7] new transparent metal oxide,[8] functional carbon materials,[9,10] metal nanowires,[11-13] and metal grids[14]. Among them, conducting polymer poly(3,4-ethylenedioxythiophene):poly(styrenesulfonate) (PEDOT:PSS, PH1000) has been considered as a promising candidate to replace ITO due to its good optical transparency, solution processability, and good mechanical flexibility. Moreover, it can be applied to top transparent electrode by film-transfer method. The high content of insulating species PSS in pristine PEDOT:PSS always leads to a low conductivity. Doped and post-treatment with various materials, such as organic solvents,[15,16] surfactant,[17,18] zwitterion,[19] sulfuric acid[7] are found to have dramatically enhanced the conductivity of PEDOT:PSS. PEDOT:PSS doped with acid treated carbon nanotubes demonstrated to obtain high conductivity of 3264.2 S cm^{-1},[20] and the H$_2$SO$_4$ post-treated sample even has achieved the highest conductivity of 4380 S cm^{-1},[21] accomplished as anode for PSC and used transfer-printing method fabricated all-plastic electrodes.[22] Although the conductivity of PEDOT:PSS has improved through above mentioned methods, most of the treatment process suffer from the difficulty to perform.

3

Ionic liquids are organic/inorganic salts with negligible vapor pressure, good chemical stability and low flammability. Dobbelin et al. reported an increase of conductivity by adding ionic liquid to PEDOT:PSS[23]. Later, Badre et al. have studied the influence of several ionic liquids on the conductivity of PEDOT:PSS[24] and found that addition of 1-ethyl-3-methylimidazolium tetracyanoborate to PEDOT:PSS can remarkably improve the conductivity to a high value of 2084 S cm^{-1}. They demonstrated that the conductivity enhancement resulted from a depletion of insulating PSS and the formation of highly conductive PEDOT domains. Liquid-crystalline ionic liquids (LCILs), a classic of ionic liquids with liquid crystalline property, not only possess the high conductivity of ionic liquid, but also present the spontaneous orientation of molecules, which can further optimize the conductivity. For example, liquid-crystalline ionic liquid 1-hexadecyl-3-methylimidazolium hexafluorophosphate ([C$_{16}$MIm]PF$_6$) shows the increased conductivity upon heating, with 2.6×10^3 S cm^{-1} at 100 °C and 2.5×10^3 S cm^{-1} at 120 °C.[25] The LCILs may induce PEDOT to form ordered microstructure, resulting in increase of the conductivity of the PEDOT:PSS. Inspired by this, herein, two LCILs, [C$_{16}$MIm]PF$_6$ and 1-hexadecyl-3-methylimidazolium tetrafluoroborate ([C$_{16}$MIm]BF$_4$) are employed to modify PEDOT:PSS (PH1000) films as transparent anodes (PH1000/LCIL) for high performance ITO-free devices (the devices architectures, chemical structures of two LCILs are shown in Figure 1). Spin-coating LCILs solution on surface of PH1000 films can effectively reduce the content of insulating PSS on top of PH1000 films, favoring assembly of PEDOT with ordered microstructure. The spontaneous orientation of the LCILs with liquid crystalline property can further promote the ordered, continuously molecular packing of PEDOT, resulting in a dramatically improved conductivity of LCIL modified PH1000 electrode. Meanwhile, LCILs in the interface of the anode and active layer can also increase crystallinity of upper active layer. As a result, ITO-free devices with PH1000/LCILs as transparent anode has realized a significantly improved performance compared with the one with pristine PH1000. In addition, the better energy alignment developed PH1000/LCILs anode

can further simplify the ITO-device structure without incorporation of any extra hole transport layer (HTL).

2. Results and Discussion

Filtered PH1000 was spin-coated on glass by 1000 rpm for 60 s, and the obtained film with thickness about 80 nm was annealed on a hot plate in ambient atmosphere at 120 ℃ for 20 min. Then, the liquid-crystalline ionic liquids (LCILs) [C_{16}MIm]PF_6 or [C_{16}MIm]BF_4 with a concentration of 1.75 mg mL^{-1} (in DMF) were spin-coated on the dried PH1000 films to prepare LCILs modified PH1000 films, followed by annealing on a hot plate in ambient atmosphere 25 ℃ for 25 min. The details of fabrication are described in the experimental section. Figure S1 compares the transmittance of PH1000, PH1000/[C_{16}MIm]PF_6 and PH1000/[C_{16}MIm]BF_4 films on quartz substrate. LCILs modified PH1000 films show the transmittance of approaching to 90%, similar to the untreated film, indicating that LCILs treatment has little influence on transparency of PH1000 films.

The work functions of PH1000 with and without the LCILs treatment were measured by Kelvin probe method (Figure S2 a and Table S1). The work function of the pristine PH1000 is in accordance with the reported value.[26] Comparing with that of pristine PH1000, the work function of the PH1000 with [C_{16}MIm]PF_6 and [C_{16}MIm]BF_4 modification slightly decrease. As shown in Figure S2 b, the work function value indicated that the modified film was still a good hole injection material for polymer donor (such as P3HT). The same result was also obtained by ultraviolet photoelectron spectroscopy (UPS) measurements (Figure S3 and Table S1).

The hydrophilic property of PH1000 layers before and after modification of LCILs is measured by contact angle measurements shown in Figure S4. Pristine PH1000 film shows the hydrophilic property with a contact angle of 64°. When PH1000 film is modified by LCILs of [C_{16}MIm]PF_6 and [C_{16}MIm]BF_4, the contact angles are enhanced to 80° and 78°, respectively, due to the hydrophobic property of the LCILs.

The hydrophobic surface can promote the formation of intimate contact between electrode and active layer, and protect the device out of oxygen and water attack, consequently leading to the improved charge injection and device stability.

Since the LCILs can influence the conductivity of the PEDOT:PSS, four point probe was performed to investigate the conductivity change of the PH1000 before and after LCILs modification. The pristine PH1000 shows an electrical conductivity of 0.4 S cm^{-1} with a high sheet resistance of 3.15×10^5 f sq^{-1}. After modified by LCILs, the conductivity of PH1000/[C$_{16}$MIm]PF$_6$ remarkably increase to 1457.7 S cm^1 with a sharply dropped sheet resistance of 98 f sq^{-1}. And [C$_{16}$MIm]BF$_4$ also exerts the similar influence on the conductivity of PH1000, that PH1000/[C$_{16}$MIm]BF$_4$ achieves an improved conductivity of 1243.8 S cm^1 with a reduced sheet resistance of 134 f sq^{-1}. (Figure 2 and Table S2).

To explore the conductivity enhancement and find out the role of LCILs, the nature of the liquid crystal was observed by the polarized optical microscopy (POM) (Figure S5). Compared to pristine PH1000 film without any birefringence, PH1000/LCIL films show obvious bright liquid crystal phase, illustrating an ordered packing arrangement of the molecule. Such ordered molecular packing is very helpful for the enhancement of the film conductivity. Moreover, the liquid crystal phase in PH1000/[C$_{16}$MIm]PF$_6$ film is brighter than that in the PH1000/[C$_{16}$MIm]BF$_4$ film, indicating a better liquid crystalline property. As a result, the PH1000/[C$_{16}$MIm]PF$_6$ has the higher conductivity than PH1000/[C$_{16}$MIm]BF$_4$.

Besides liquid crystalline property, the substantially morphological change is also found to be an important factor for the conductivity enhancement. Figure 3 shows the atomic force microscope (AFM) topography of a 5 µm×5 µm of the area of the pristine PH1000 film and PH1000/LCIL films. In AFM images, all of the films have quite smooth surface, the bright region is associated with PEDOT domains and the dark regions denote the soft structure arising from excess PSS. After LCILs

modification, the dark PSS regions of the PH1000 decrease, while the bright PEDOT regions increase and become continuous, interpreting that some of the insulating PSS chains in PH1000 film surface has been removed during spin-coating of the LCILs on PH1000. The enrichment of continuous PEDOT domains on PH1000 film surface can provide the efficient conducting channels for charges, which should be responsible for the enhancement in the conductivity of the modified PH1000 films. This results are consistent with the literature.[24] In addition, with respect to PH1000/[C$_{16}$MIm]BF$_4$ film, [C$_{16}$MIm]PF$_6$ treated films shows more larger PEDOT domains (bright domains), thereby causing a further enhancement in the conductivity. The improved morphology and conductivity of the PH1000/LCIL electrode would be favorable for the improvement of the photovoltaic performance.

The morphological change of the LCILs modified PH1000 originating from enrichment of PEDOT by the removal of PSS has been further confirmed by X-Ray photoelectron spectroscopy (XPS) measurement. Figure 4a and b shows S(2p) and F(1s) XPS spectra of the PH1000 films before and after LCILs treatment. As shown in Figure 4a, the S(2p) peaks observed at the binding energy of 168.0 eV corresponds to the sulfur signal of SO$_3$H from PSS, while the peaks at the 164.7 eV and 163.5 eV assign to the sulfur signal from PEDOT. From the figure we can see that the intensity of peaks of PEDOT after LCILs modification is much stronger than that of unmodified one, especially for the [C$_{16}$MIm]PF$_6$ modified film. The ratio of PEDOT to PSS in PH1000 solution is about 1:2.5, but the calculated ratio of PEDOT to PSS in the PH1000 film is 1:4.79, due to that PSS tends to aggregate on the film surface resulting in a higher content of PSS on the surface than in the bulk.[28,29] However, the ratio of PEDOT to PSS sharply increased to 1:2.36 for the PH1000/[C$_{16}$MIm]PF$_6$ film and 1:2.86 for the PH1000/[C$_{16}$MIm]BF$_4$ film, with 51% and 40% reduction of PSS from the film surface, respectively. Moreover, the peaks of the PEDOT shift to lower binding energy, indicative of a strong interaction in the film after modification. These results suggest that half of PSS has been successfully removed and replaced by LCILs due to the interaction between anion group of LCILs and thiophene units of PEDOT. The removal of the insulator PSS from PH1000 film surface helps formation of

continuous PEDOT domains and increases conductivity of the LCILs-modify PH1000 films. As shown in Figure 4b, the peaks of F(1s) can be clearly observed at 686 of the PH1000/[C$_{16}$MIm]PF$_6$ film. Table S3 showed the content of F atom on films. Compared to the pristine PH1000 film (0.06%), the content of F atom is 0.65% and 0.12% on the surface of the PH1000/[C$_{16}$MIm]PF$_6$ and PH1000/[C$_{16}$MIm]BF$_4$ film, respectively. The content of F atom of the pristine PH1000 film is much lower than that of the modification film. So the F signal of the pristine film must come from measurement error. These proved the liquid-crystalline ionic liquids stay on the surface of PEDOT:PSS after spin coating, and the amount of [C$_{16}$MIm]PF$_6$ staying on the surface of the films should be larger than that of [C$_{16}$MIm]BF$_4$. To investigate the liquid-crystalline ionic liquids acting on the films during spin coating, depth profiling of XPS was carried out. Figure 4c and e show that the S(2p) peaks of PSS in the films after 60 s and 120 s sputtering are obviously decreased in comparison to the films without etching treatment. Table S3 and Figure 4d and f show that the F(1s) peaks completely disappeared in both pristine PH1000 film and PH1000/[C$_{16}$MIm]BF$_4$ film after 60 s and 120 s sputtering. But the content of F atom is 0.34% and 0.31% in the PH1000/[C$_{16}$MIm]PF$_6$ films after etching for 60 s and 120 s, respectively. Therefore, it is concluded that [C$_{16}$MIm]PF$_6$ not only affect the surface of PH1000 film, but also act on bulk of the film, but the [C$_{16}$MIm]BF$_4$ modification only affect on the surface of the PH1000 film. The results of XPS depth profiling indicated that [C$_{16}$MIm]PF$_6$ may induce PEDOT to form continuous, ordered microstructure of the film.

To gain deeper insight into the morphology change of the PH1000 caused by LCILs treatment, transmission electron microscopy (TEM) was performed on all of the PH1000 films. As shown in Figure 5, the dark and bright domains are assigned to PEDOT-rich regions and PSS-rich regions in the films, respectively.[30] The pristine PH1000 has a lot of non-continuous dark nanofibrils and dots attributing to PEDOT film (Figure 5a). In PH1000/[C$_{16}$MIm]PF$_6$ (Figure 5b) and PH1000/[C$_{16}$MIm]BF$_4$ (Figure 5c) films, dark domains increase and bright domains decrease. Moreover, dark nanofibrils become more distinct in PH1000/[C$_{16}$MIm]PF$_6$ than in

PH1000/[C$_{16}$MIm]BF$_4$. It indicates that LCILs can induce PEDOT to form ordered microstructure and favorable molecular packing. The continuous and ordered nanofibrils of PEDOT should contribute to the dramatically enhanced conductivity of the films. The ordered microstructure and favorable molecular packing also can be discerned by X-ray diffraction (XRD) patterns (Figure S6). The low angle reflections at 2θ=3.3° and 6.4° correspond to the lamella stacking distance d(100), two distinct alternate orderings of PEDOT and PSS,[31] whereas the two high angle reflections at 2θ=17.8° and 25.6° are indexed to the amorphous halo of PSS and the interchain planar ring-stacking distance d(010) of PEDOT, respectively.[21] After PH1000 films modified by LCILs, the peak at 2θ=3.3° shows an increased intensity in the XRD spectra, indicating the improved crystallinity of PEDOT in PH1000/LCIL films. From the POM, AFM, TEM and XRD results, the mechanism of microstructure of PH1000 induced by LCILs can be schematically illustrated in Figure 5d.

The highly conductive and transparent LCILs modified PH1000 films were applied as the transparent anode in PSC devices with a wide studied and stable donor:acceptor blend of poly(3-hexylthiophene) (P3HT) and [6,6]-phenyl-C$_{61}$-butyric acid methyl ester (PC$_{61}$BM) as active layer. The conventional structure is glass/PH1000/LCIL/P3HT:PC$_{61}$BM/LiF/Al with devices effective area of 18 mm^2. Figure S7 presents the current density vs. voltage (J-V) characteristics of conventional devices under AM 1.5G illumination at an irradiation intensity of 100 mW cm^{-2}, and related parameters are summarized in Table 1. When the pristine PH1000 film is used as transparent anode, the device exhibits very poor photovoltaic performance because of its high series resistance (R_s) and an associated extremely low conductivity. However, incorporation of the PH1000/[C$_{16}$MIm]PF$_6$ anode into the device achieves the highest power conversion efficiency (PCE) of 2.50%, with a short-current density (J_{sc}) of 6.22 mA cm^{-2}, an open-circuit voltage (V_{oc}) of 0.60 V, and an fill factor (FF) of 66.5%. This value is even higher than that of ITO-based device (2.40%). PH1000/[C$_{16}$MIm]BF$_4$ based device also yields the equal PCE to the ITO-based one (2.40% vs 2.40%). It is worthy to note that different from the

efficiency obtained from the ITO-based device, the decent PCE from PH1000/LCIL is without incorporation of the P VP AI 4083 as hole-transporting layer (HTL). Figure S7 also compares the J-V curves and related parameters of devices base on PH1000/LCILs electrode with and without P VP AI 4083 HTL. Inserting a layer of P VP AI 4083 HTL into the devices based on PH1000/LCILs electrode results in a significant decrease in the PCE together with a dramatic drop in FF. From the Table 1 we also can see that compared with the devices with P VP AI 4083 HTL, the ones only with PH1000/LCIL shows relatively lower R_S and higher shunt resistance (R_{SH}) values. The work function of the PH1000/LCILs electrode is high enough to match well with active layer. Meanwhile, as seen from the SEM image (Figure S8), the hydrophobic PH1000/LCIL film covered by the highly hydrophilic P VP AI 4083 film exhibit a relatively coarse surface, showing that the P VP AI 4083 does not facilitate the formation of homogeneous films. Therefore, without incorporation of extra HTL, the LCIL-modified PH1000 electrode could realize a favorable energy alignment in the device. Enabling the simplified ITO-free device structure by LCIL-modified PH1000 electrode is compatible with the large scale commercial production.

The electrical conductivity of the PH1000 modified by LCILs is higher than that of the pristine PH1000, but lower than that of ITO. However, the PCE of the ITO-free device base on PH1000/[C_{16}MIm]PF$_6$ as transparent anodes is higher than that of device base on ITO anode (Figure S7 and Table 1). As reported earlier, the orientation of LCILs can enhance the crystallization of P3HT.[32] To further elucidate the effect of the PH1000/LCIL on improvement of photovoltaic performance, the morphology change of the active layer induced by LCILs is determined. The TEM images of the P3HT:PC$_{61}$BM films are shown in Figure 6. As Compared with the morphology of P3HT:PC$_{61}$BM films on pristine PH1000 (Figure 6a) and PH1000/LCIL (Figure 6b and c), the active layer deposited on the PH1000/[C_{16}MIm]PF$_6$ (Figure 6b) and PH1000/[C_{16}MIm]BF$_4$ (Figure 6c) exhibit distinct nanofibrils in the TEM images. The formation of nanofibrils should be ascribed to the improved crystallization of P3HT induced by the orientation of LCILs,

thereby, the carrier transport can be improved. To further demonstrate this point, a small amount of LCILs (1mg/mL) was directly blended with the P3HT and $PC_{61}BM$. As revealed by the TEM image of P3HT:PC_{61}BM:[C_{16}MIm]PF_6 (Figure S9a) and P3HT:PC_{61}BM:[C_{16}MIm]BF_4 (Figure S9b) films spin-coated on the pristine PH1000, both of them form similar nanofibril morphology. These findings prove that due to the orientation of liquid crystalline molecules, LCILs at the interface of the PH1000 and active layer can induce the self-assembly of both PEDOT and the P3HT to improve their crystallization, thus contributing to the PCE enhancement.

To investigate the validity of the PH1000/LCIL films as transparent anode in different active layer materials, the device based on low bandgap donor material such as thieno[3,4b]-thiophene/benzodithiophene (PTB7) blended with [6,6]-phenyl C_{71}-butyric acid methyl ester (PC_{71}BM) were fabricated. The cathode interlayer material is poly [(9,9-bis(3´-(N,N-dimethylamino) propyl)-2,7-fluorene)-alt-2,7-(9,9-dioctylfluorene)] (PFN). The conventional structure is glass/anode/PTB7:PC_{71}BM/PFN/Al with devices effective area of 18 mm^2. The J-V curves and photovoltaic parameters of PTB7:PC_{71}BM devices based on the PH1000/LCIL and pristine ITO transparent anode are shown in Figure 7a and Table 1, respectively. The PCEs of the devices with PH1000/LCIL electrodes are slightly lower than that from the device with traditional ITO electrode (5.5%). The slight inferior performance of PH1000/LCIL-based device compared to that of ITO-based one is mainly due to the slight decreases of both J_{sc} and V_{oc}. However, the efficiency still shows relatively high PCE 4.6% for PH1000/[C_{16}MIm]PF_6 and 4.5% for PH1000/[C_{16}MIm]BF_4. This suggests that PH1000/LCIL is an universal electrode to replace ITO for high performance PSCs. Furthermore, the IPCE spectra in Figure 7b is in good accordance with the J_{sc} values.

3. Conclusions

In summary, two highly conductive LCILs [C_{16}MIm]PF_6 and [C_{16}MIm]BF_4 have been successfully incorporated in ITO-free PSCs by spin-coating on the surface PH1000

films as transparent anodes for high performance PSCs. LCILs modification can remove half of the insulating PSS on top surface of the PH1000 and induce the formation of PEDOT with ordered and continuous molecular packing. At the same time, spontaneous orientation of the LCILs with liquid crystalline property can further promote the ordered packing arrangement of both PH1000 and active layer. As a result, compared to the pristine PH1000, the LCILs modified PH1000 possesses dramatically improved conductivity. Consequently, a high performance ITO-free device based on LCIL-modified PH1000 anode without extra HTL has been realized. It also should be noted that PH1000/LCIL has a universal application as anode for versatile ITO-free devices. These findings indicate that solution-processed PH1000/LCIL electrode shows great potential applications in the fabrication of highly efficient PSCs as well as large-area, flexible printed PSCs.

4. Experimental Section

Materials: PEDOT:PSS aqueous solutions (PH1000) was bought from Heraeus Ltd. with a PEDOT:PSS concentration of 1.3 wt% by weight dispersed in H_2O. 1-hexadecyl-3-methylimidazolium hexafluorophosphate ([C$_{16}$MIm]PF$_6$) and 1-hexadecyl-3-methylimidazolium tetrafluoroborate ([C$_{16}$MIm]BF$_4$) were bought from Energy Chemical and the center for green chemistry, LICP, CAS respectively. The P3HT (4200E) was bought from Rieke Metals Inc and PC$_{61}$BM (99.5%) were bought from American Dye Source, Inc. The PTB7 and PC$_{71}$BM were purchased from 1-material Chemscitech Inc. (St-Laurent, Quebec, Canada) and Solarmer Energy Inc respectively. All purchased materials were used as received.

Preparation characterization of PH1000 and PH1000/LCIL films: Glass substrates of area 1.5×1.5 cm^2 were successively cleaned in acetone, detergent water, thrice deionized water for 15 min each and isopropyl alcohol by ultrasonic agitation, and then dried in N_2. PH1000 filtered through a 0.45 μm syringe filter was spin-coated at 1000 rpm for 60 s on glass which were treated with UV for 20 minutes prior to spin coating. The obtained films (thickness 80 nm) were annealed on hot plate in ambient atmosphere at 120 °C for 20 min. By spin-coated LCIL DMF solution

(1.75 mg mL^{-1}) on the dried PH1000 films at 2000 rpm for 60 s to afford the PH1000/LCIL films, Then the modified films were annealed on a hot plate in ambient atmosphere at 120 °C for 25 min. The PH1000/[C$_{16}$MIm]PF$_6$ films with a thickness about of 70 nm, and the PH1000/[C$_{16}$MIm]BF$_4$ films with a thickness about of 60 nm. The thickness of [C$_{16}$MIm]PF$_6$ layer and [C$_{16}$MIm]BF$_4$ is about of 20 nm and 10 nm, respectively.

Fabrication of PSCs PSCs devices were fabricated using PH1000 and PH1000/LCIL films as the transparent anodes on glass, and P3HT:PC$_{61}$BM, PTB7:PC$_{71}$BM were chosen as active layer for comparison. The P3HT:PC$_{61}$BM (1:1 by weight) active blend layer with a thickness of 100 nm was prepared by spincoating the dichlorobenzene (DCB) solution at 800 rpm for 30 s and then 1400 rpm for 2 s. The devices are annealed at 150 °C for 10 min on hotplate in a glove box. The PTB7:PC$_{71}$BM (1:1.5 by weight) active blend layer were prepared by spincoating mixed solvent of chlorobenzene : 1,8-diiodoctane (97:3 by volume) solution at 1000 rpm 2 min. The cathode interlayer material poly [(9,9-bis(3′-(N,N-dimethylamino) propyl)-2,7-fluorene)-alt-2,7-(9,9-dioctylfluorene)] (PFN) was dissolved in methanol under the presence of small amount of acetic acid 0.1 mg/mL was spincoated onto the top of the obtained active layer at 5000 rpm for 60 s to form a thin interlayer. Then 100 nm Al is evaporated through a shadow mask under 10^{-5}.

Supporting Information

The detailed experimental sections, transmittance, the work function measurement, the contact angle measurement, the electrical property of the films, polarized optical micrographs of the films, F atom content of films surface, X-ray diffractograms, J-V curves of P3HT:PC$_{61}$BM BHJ-PSC devices, SEM images and TEM images of P3HT:PC$_{61}$BM blend with LCIL are in Supporting Information. This information is available free of charge via the Internet at http://pubs.acs.org.

Acknowledgements

References

(1)   Forrest, S. R. The path to ubiquitous and low-cost organic electronic appliances on plastic. Nature 2004, 428, 911-918.

(2)   Park, H. J.; Kang, M. G.; Ahn, S. H.; Guo, L. J. A Facile Route to Polymer Solar Cells with Optimum Morphology Readily Applicable to a Roll-to-Roll Process without Sacrificing High Device Performance. Adv. Mater. 2010, 22, E247-E253.

(3)   Liu, Y. H.; Zhao, J. B.; Li, Z. K.; Mu, C.; Ma W.; Hu, H. W.; Jiang, K.; Lin, H. R.; Ade, H.; Yan, H. Aggregation and morphology control enables multiple cases of high-efficiency polymer solar cells. Nat. Commun. 2014, 5, 5293-5300.

(4)   He, Z. C.; Xiao, B.; Liu, F.; Wu, H. B.; Xiao, S.; Wang, C.; Russell, T. P.; Cao, Y. Single-junction polymer solar cells with high efficiency and photovoltage. Nat. Photon. 2015, 9, 174-179.

(5)   Inganäs, O. Organic photovoltaics: Avoiding indium. Nat. Photon. 2011, 5, 201~202.

(6)   Ouyang, J.; Yang, Y. Conducting polymer as transparent electric glue. Adv. Mater. 2006, 18, 2141, 2144.

(7)   Xia, Y. J.; Sun, K.; Ouyang, J. Y. Solution-Processed Metallic Conducting Polymer Films as Transparent Electrode of Optoelectronic Devices. Adv. Mater. 2012, 24, 2436-2440.

(8)   Hagendorfer, H.; Lienau, K.; Nishiwaki, S.; Fella, C. M.; Kranz, L.; Uhl, A. R.; Jaeger, D.; Luo, L.; Gretener, C.; Buecheler, S.; et.al. Highly Transparent and Conductive ZnO: Al Thin Films from a Low Temperature Aqueous Solution Approach. Adv. Mater. 2014, 26, 632-636.

(9)   Tung, V. C.; Chen, L. M.; Allen, M. J.; Wassei, J. K.; Nelson, K.; Kaner, R. B.; Yang, Y. Low-Temperature Solution Processing of Graphene, Carbon Nanotube

Hybrid Materials for High-Performance Transparent Conductors. Nano Letters, 2009, 9, 1949–1955.

(10) Konios, D.; Petridis, C.; Kakavelakis, G.; Sygletou, M.; Sawa, K.; Stratakis, E.; Kymakis, E. Reduced Graphene Oxide Micromesh Electrodes for Large Area, Flexible, Organic Photovoltaic Devices. Adv. Funct. Mater. 2015, DOI: 10.1002/adfm.201404046.

(11) Yang, L. Q.; Zhang, T.; Zhou, H. X.; Price, S. C.; Wiley, B. J.; You, W. Solution-Processed Flexible Polymer Solar Cells with Silver Nanowire Electrodes. ACS Appl. Mater. Interfaces 2011, 3, 4075–4084.

(12) Guo, F.; Zhu, X. D.; Forberich, K.; Krantz, J.; Stubhan, T.; Salinas, M.; Halik, M.; Spallek, S.; Butz, B.; Spiecker, E.; et. al. ITO-Free and Fully Solution-Processed Semitransparent Organic Solar Cells with High Fill Factors. Adv. Energy Mater. 2013, 3, 1062–1067.

(13) Jin, Y. X.; Li, L.; Cheng, Y. R.; Kong, L.Q.; Pei, Q. B.; Xiao, F. Cohesively Enhanced Conductivity and Adhesion of Flexible Silver Nanowire Networks by Biocompatible Polymer Sol–Gel Transition. Adv. Funct. Mater. 2015, 25, 1581–1587.

(14) Han, B.; Pei, K.; Huang, Y. L.; Zhang, X. J.; Rong, Q. K.; Lin, Q. G.; Guo, Y. F.; Sun, T. Y.; Guo, C. F.; Carnahan, D. et a1. Uniform Self-Forming Metallic Network as a High-Performance Transparent Conductive Electrode. Adv. Mater. 2014, 26, 873–877.

(15) Kim, Y. H.; Sachse, C.; Machala, M. L.; May, C.; Müller-Meskamp, L.; Leo, K. Highly Conductive PEDOT:PSS Electrode with Optimized Solvent and Thermal Post-Treatment for ITO-Free Organic Solar Cells. Adv. Funct. Mater. 2011, 21, 1076–1081.

(16) Alemu, D.; Wei, H. Y.; Ho, K. C.; Chu, C. W. Highly Conductive PEDOT:PSS Electrode by Simple Film Treatment with Methanol for ITO-Free Polymer Solar Cells. Energy Environ. Sci. 2012, 5, 9662–9671.

(17) Vosgueritchian, M.; Lipomi, D. J.; Bao, Z. A. Highly Conductive and Transparent PEDOT:PSS Films with a Fluorosurfactant for Stretchable and

Flexible Transparent Electrodes. *Adv. Funct. Mater.* **2012**, *22*, 421-428.

(18) Zhang, W. F.; Zhao, B. F.; He, Z. C.; Zhao, X. M.; Wang, H. T.; Yang, S. F.; Wu, H. B.; Cao, Y. High-Effciency ITO-Free Polymer Solar Cells Using Highly Conductive PEDOT:PSS/surfactant Bilayer Transparent Anodes. *Energy Environ. Sci.* **2013**, *6*, 1956-1964.

(19) Xia, Y. J.; Zhang, H. M.; Ouyang, J. Y. Highly Conductive PEDOT:PSS Films Prepared Through a Treatment with Zwitterions and Their Application in Polymer Photovoltaic Cells. *J. Mater. Chem.* **2010**, *20*, 9740-9747.

(20) Hu, X. T.; Chen, L.; Zhang Y.; Hu, Q.; Yang J. L.; Chen Y. W. Large-scale Flexible and Highly Conductive Carbon Transparent Electrodes via Roll-to-roll Process and Its High Performance Lab-scale ITO-free PSCs. *Chem. Mater.* **2014**, *26*, 6293-6302.

(21) Kim, N.; Kee, S.; Lee, S. H.; Lee, B. H.; Kahng, Y. H.; Jo, Y. R.; Kim, B. J.; Lee, K. Highly Conductive PEDOT:PSS Nanobrils Induced by Solution-Processed Crystallization. *Adv. Mater.* **2014**, *26*, 2268-2272.

(22) Kim, N.; Kang H.; Lee J. H.; Kee S.; Lee S. H.; Lee K. Highly Conductive All-Plastic Electrodes Fabricated Using a Novel Chemically Controlled Transfer-Printing Method. *Adv. Mater.* **2015**, DOI: 10.1002/adma.201500078

(23) Dobbelin, M.; Marcilla, R.; Salsamendi, M.; Pozo-Gonzalo, C.; Carrasco, P. M.; Mecerreyes, D. Influence of Ionic Liquids on the Electrical Conductivity and Morphology of PEDOT:PSS Films. *Chem. Mater.* **2007**, *19*, 2147-2149.

(24) Badre, C.; Marquant, L.; Alsayed, A. M.; Hough, L. A. Highly Conductive Poly(3,4-ethylenedioxythiophene):Poly(styrenesulfonate) Films Using 1-Ethyl-3-methylimidazolium Tetracyanoborate Ionic Liquid. *Adv. Funct. Mater.* **2012**, *22*, 2723-2727.

(25) Roche, J. D.; Gordon, C. M.; Imrie, C. T.; Ingram, M. D.; Kennedy, A. R.; Celso, F. L.; Triolo, A. Application of Complementary Experimental Techniques to Characterization of the Phase Behavior of [C_6mim][PF_6] and [C_{14}mim][PF_6]. *Chem. Mater.* **2003**, *15*, 3089-3097.

(26) Zhou, Y. H.; Cheun, H.; Choi, S.; Potscavage, W. J. Jr.; Fuentes-Hernandez, C.;

Kippelen, B. Indium Tin Oxide-Free and Metal-Free Semitransparent Organic Solar Cells. Appl. Phys. Lett. 2010, 97, 153304

(27) Peng, B.; Guo, X.; Cui, C. H.; Zou, Y. P.; Pan, C. Y.; Li, Y. F. Performance Improvement of Polymer Solar Cells by Using a Solvent-Treated Poly(3,4-ethylenedioxythiophene)-Poly(styrenesulfonate) Buffer Layer. Appl. Phys. Lett. 2011, 98, 243308.

(28) Lee, T. W.; Chung, Y. S. Control of the Surface Composition of a Conducting Polymer Complex Film to Tune the Work Function. Adv. Funct. Mater. 2008, 18, 2246-2252

(29) Na, S. I.; Wang, G.; Kim, S. S.; Kim, T. W.; Oh, S. H.; Yu, B. K.; Lee, T.; Kim, D. Y. Evolution of Nanomorphology and Anisotropic Conductivity in Solvent-Modified PEDOT:PSS Films for Polymeric Anodes of Polymer Solar Cells. J. Mater. Chem. 2009, 19, 9045-9053

(30) Hsiao, Y. S.; Whang, W. T.; Chen, C. P.; Chen, Y. C. High-conductivity poly(3,4-ethylenedioxythiophene):poly(styrene sulfonate) film for use in ITO-free polymer solar cells. J. Mater. Chem. 2008, 18, 5948-5955.

(31) Kim, N.; Lee, B. H.; Choi, D.; Kim, G.; Kim, H.; Kim, J. R.; Lee, J.; Kahng, Y. H.; Lee, K. Role of Interchain Coupling in the Metallic State of Conducting Polymers. Phys. Rev. Lett. 2012, 109, 106405-106409.

(32) Zhou, W. H.; Shi, J. M.; Lv, L. J.; Chen, L.; Chen, Y. W. A mechanistic investigation of morphology evolution in P3HT-PCBM films induced by liquid crystalline molecules under external electric field. Phys. Chem. Chem. Phys. 2015, 17, 387-397.

Figure 1 a) Device architectures of the ITO-free BHJ PSC devices using PH1000/LCIL films as the transparent anode, the chemical structures of LCIL b) $[C_{16}MIm]PF_6$ and c) $[C_{16}MIm]BF_4$.
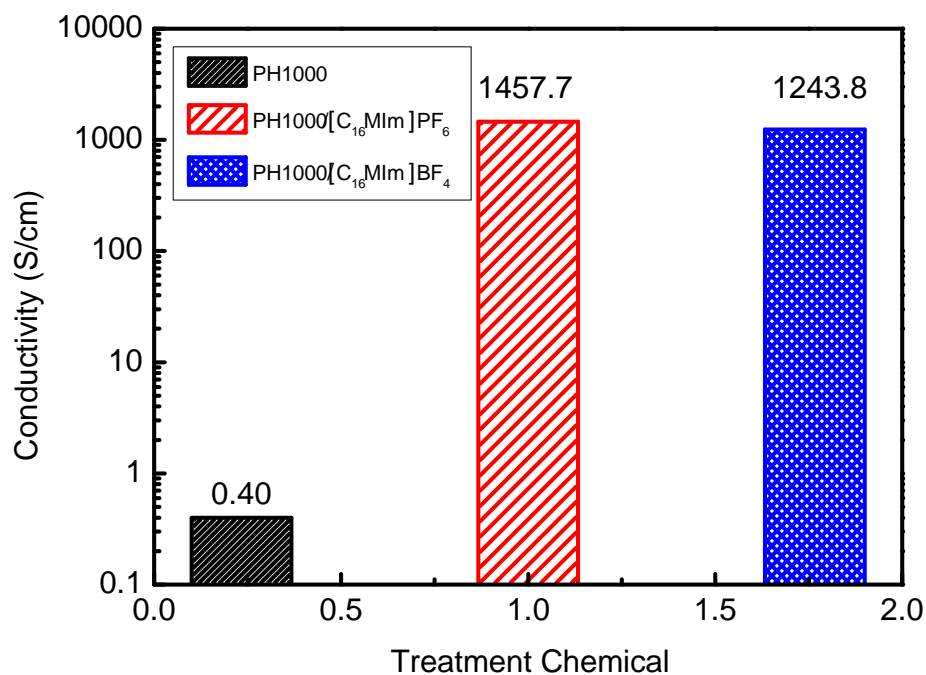
Figure 2 Conductivities of pristine PH1000 film, [C$_{16}$MIm]PF$_6$ or [C$_{16}$MIm]BF$_4$ modified PH1000 films.

Figure 3 AFM topography image of film (a) PH1000 film; (b) PH1000/[C$_{16}$MIm]PF$_6$ film and (c) PH1000/[C$_{16}$MIm]BF$_4$ film. All the images are 5μm×5μm.
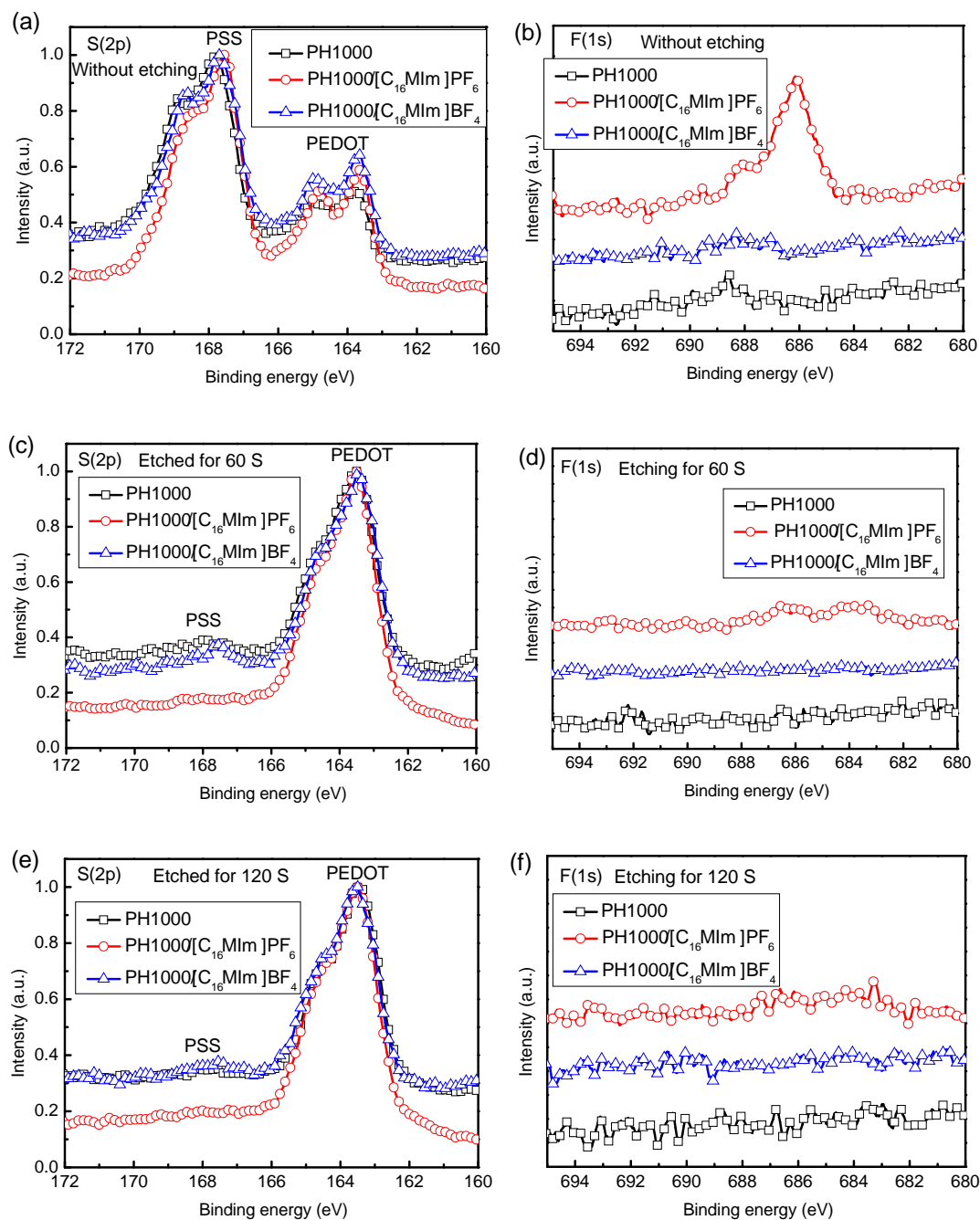
Figure 4 The S(2p) XPS spectra of pristine PH1000 film, [C$_{16}$MIm]PF$_6$ or [C$_{16}$MIm]BF$_4$ modified PH1000 film (a) without etching, (c) after etching for 60 s, (e) after etching for 120 s, The F(1s) XPS spectra of pristine PH1000 film, [C$_{16}$MIm]PF$_6$ or [C$_{16}$MIm]BF$_4$ modified PH1000 film (b) without etching, (d) after etching for 60 s, (f) after etching for 120 s.

Figure 5 TEM topography image of (a) pristine PH1000 film, and (b) [C$_{16}$MIm]PF$_6$ and (c) [C$_{16}$MIm]BF$_4$ modified PH1000 film, respectively. (d) Schematic illustration of the mechanism of Microstructure of PH1000 Induced by LCILs.

Table 1 Summary of the Photovoltaic performance of P3HT:PC$_{61}$BM or PTB7:PC$_{71}$BM Solar Cells with Various transparent anodes. All devices with an effective area of 18 mm^2

Devices(18 mm^2)	Jsc (mA cm^{-2})	Voc (V)	FF (%)	PCE (%)	Average PCE (%)	Rs(‡ cm^2)	Rsh (‡ cm^2)
Glass/ITO/ P VP AI 4083/P3HT:PC$_{61}$BM/LiF/Al	6.15	0.62	63.0	2.4	2.35	4.84	17?0.4
Glass/PH1000/P3HT:PC$_{61}$BM/LiF/Al	0.33	0.59	25.4	0.05	0.03	1549.9	17??.8
Glass/PH1000/[C$_6$MIm]PF$_6$/P3HT:PC$_{61}$BM/LiF/Al	6.22	0.60	66.5	2.5	2.50	4.6	16??.8
Glass/PH1000/[C$_6$MIm]PF$_6$/P VP AI 4083/P3HT:PC$_{61}$BM/LiF/Al	6.37	0.62	52.6	2.1	2.05	16.7	97?.7
Glass/PH1000/[C$_6$MIm]BF$_4$/P3HT:PC$_{61}$BM/LiF/Al	6.46	0.61	60.3	2.4	2.35	5.9	62?6
Glass/PH1000/[C$_6$MIm]BF$_4$/P VP AI 4083/P3HT:PC$_{61}$BM/LiF/Al	6.16	0.61	53.8	2.0	1.90	7.0	5??0
Glass/ITO/P VP AI 4083/PTB7:PC$_{71}$BM/PFN/Al	12.54	0.73	60.0	5.5	5.35	4.36	46??.06
Glass/PH1000/[C$_6$MIm]PF$_6$/PTB7:PC$_{71}$BM/PFN/Al	10.54	0.72	60.3	4.6	4.50	8.48	37?.?3
Glass /PH1000/[C$_6$MIm]BF$_4$/PTB7:PC$_{71}$BM/PFN/Al	11.19	0.72	56.1	4.5	4.35	9.18	39?.75

Figure 6 TEM images of P3HT:PC$_{61}$BM films obtained from spincoated on (a) the pristine PH1000, the PH1000 film modified with (b) [C$_{16}$MIm]PF$_6$ and (c) [C$_{16}$MIm]BF$_4$.
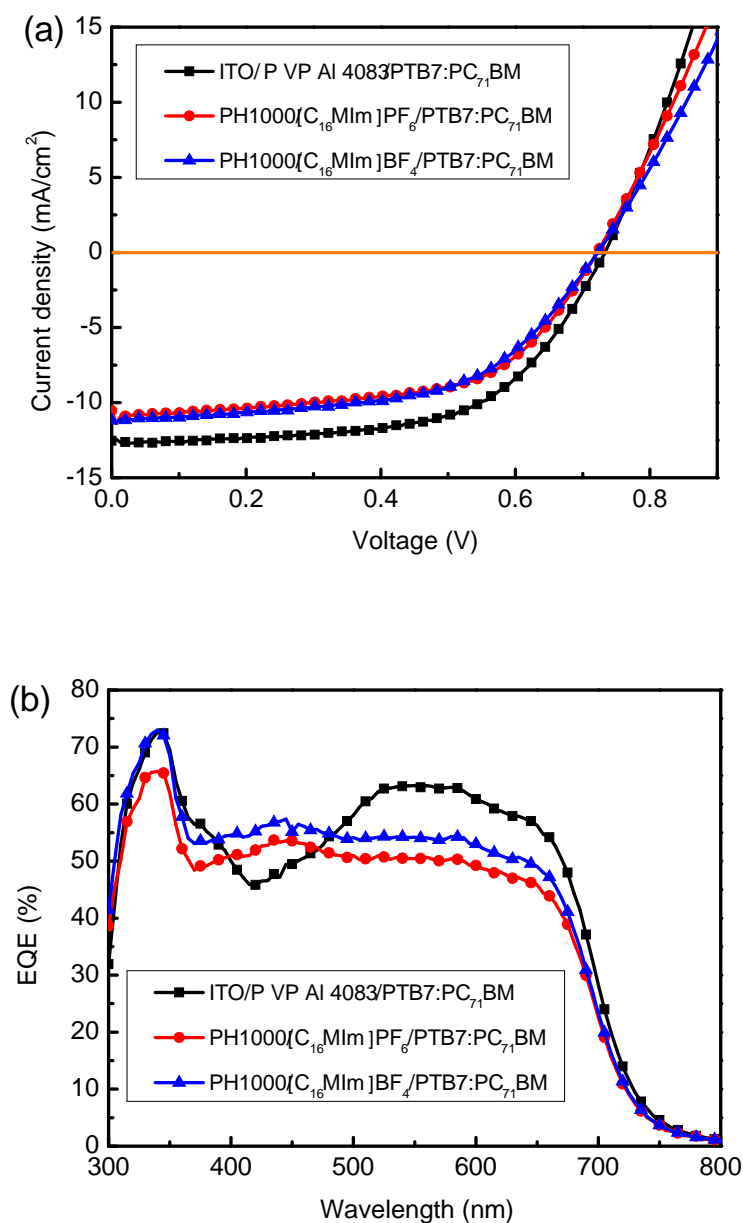
Figure 7 (a) J-V curves of PTB7:PC$_{71}$BM BHJ-PSC devices with an effective area of 18 mm^2, using ITO, PH1000/[C$_{16}$MIm]PF$_6$ and PH1000/[C$_{16}$MIm]BF$_4$ films as the transparent anodes. The measurements were carried out under AM 1.5G illumination at an irradiation intensity of 100 mW cm^{-2}. (b) IPCE spectra of the solar cells with ITO, PH1000/[C$_{16}$MIm]PF$_6$ and PH1000/[C$_{16}$MIm]BF$_4$ films as the transparent anodes base on PTB7:PC$_{71}$BM active layer.

Table of contents

Liquid -Crystalline Ionic Liquids Modified Conductive Polymers as Transparent

Electrode for Indium -Free Polymer Solar Cells

Shuqin Xiao, Lie Chen, Licheng Tan, Yiwang Chen*

Ordered microstructure and high conductivity of poly(3,4-ethylenedioxythiophene): poly-(styrene sulfonate) films for transparent anode were obtained by liquid-crystalline ionic liquids modification.

ToC figure